Society of Medical Education & Research

2025, Volume 5, Issue 2, Page No: 108-124
ISSN: 3108-4834

Archive of International Journal of Cancer and Allied Science

Proof-of-Principle for Selective Enhancement of Nucleotide Imbalance in Cancer Cells

James Robert Henderson[1]*, Kevin Alan Peterson[1], Lisa Michelle Carter[1] , David Bruce Hall[1]

[1]Kenya Department of Oncology, University of Minnesota, Minneapolis, United States.

***E-mail** ✉ j.henderson.umn@gmail.com

Abstract

Potent and selective inhibitors of dihydroorotate dehydrogenase (DHODH), a critical enzyme in the de novo synthesis of pyrimidine ribonucleotides, are being tested in clinical trials for autoimmune disorders, viral infections, and various cancers. A limitation of these DHODH inhibitors (DHODHi) is their immunosuppressive activity, which may dampen antitumor immune responses, highlighting the need for strategies that improve their therapeutic index in oncology. In this study, we explored methods to protect activated T cells from DHODH blockade and sought to identify tumor types that are particularly vulnerable to these compounds. We found that supplementing culture media with cytidine, similar to uridine, can rescue T cells from the effects of DHODH inhibition. Next, we examined cancer cells for alterations in pyrimidine biosynthesis enzyme expression and discovered that cytidine deaminase (CDA)—the enzyme responsible for converting cytidine into uridine—is expressed at low levels in a substantial fraction of cancer cell lines. CDA expression was consistently low in neuroblastoma samples and in cell lines derived from neuroblastoma and small cell lung carcinoma. These findings suggested that, under DHODHi treatment, excess extracellular cytidine could selectively impair the growth of cancer cells with low CDA expression. This hypothesis was supported by experiments showing that cytidine supplementation rapidly reduced viability in low-CDA-expressing cells cultured with fetal bovine serum, although the effect was less pronounced in human serum. Notably, CDA is present both intracellularly and in human plasma, which may influence cytidine metabolism in vivo. Using recombinant CDA, human serum, pharmacologic CDA inhibition, and T cell/cancer co-culture models, our results indicate that the therapeutic window of DHODHi could be expanded by targeting patients with low-CDA-expressing tumors while modulating extracellular cytidine levels or the cytidine-to-uridine ratio. Taken together, this proof-of-principle work supports further investigation into strategies for depleting extracellular CDA as a means to enhance the efficacy and selectivity of DHODH inhibitors in cancer therapy.

Keywords: Cancer cells, Nucleotide imbalance, DHODH, Tumor types

Introduction

Uridine monophosphate (UMP) occupies a central role in the metabolism of pyrimidine nucleotides [1]. It serves as a precursor for UTP, CTP, and thymidine nucleotides, which in turn contribute to the biosynthesis of UDP-sugars, phospholipids, RNA, and DNA. As a result, disturbances in pyrimidine nucleotide levels or imbalances among them can compromise cell proliferation and, if G1 arrest fails, generate stress during DNA replication. In mammalian cells, UMP is produced through the de novo pathway from glutamine and aspartate, as well as via the salvage pathway that utilizes circulating pyrimidine nucleosides.

Our group became interested in pyrimidine metabolism during a screen for compounds that activate p53 without inducing G2 arrest, a cell cycle block that can promote genomic instability in both normal and cancer cells [2]. Unexpectedly, many of the compounds identified were inhibitors of DHODH, the rate-limiting enzyme in de novo UMP synthesis [2-4]. Recently, several highly selective DHODH inhibitors have been developed. Some are orally available and show antitumor activity in mouse models without detectable toxicity [1, 5-9].

Access this article online https://smerpub.com/

Received: 21 May 2025; **Accepted:** 04 October 2025

How to cite this article: Henderson JR, Peterson KA, Carter LM, Hall DB. Proof-of-Principle for Selective Enhancement of Nucleotide Imbalance in Cancer Cells. Arch Int J Cancer Allied Sci. 2025;5(2):108-24. https://doi.org/10.51847/CdGbnCCX11

Translating these findings to humans requires consideration of species-specific differences. For example, plasma levels of uridine and cytidine in mice are approximately 1.2–5 μM and 1.5–3.6 μM, respectively, whereas in humans, uridine ranges from 3–5 μM and cytidine from 0.3–0.7 μM [10-13]. This demonstrates that murine plasma has higher cytidine concentrations and a higher cytidine-to-uridine ratio than human plasma, which may influence cellular responses to DHODH inhibition.

Proliferating T cells are highly sensitive to DHODH inhibition, a property exploited clinically by leflunomide and its active metabolite teriflunomide in autoimmune disorders [14]. This immunosuppressive effect, however, poses a potential challenge when considering DHODH inhibitors for cancer therapy. Therefore, strategies that protect activated T cells could improve the therapeutic window of these agents in oncology.

Our findings show that extracellular cytidine supplementation, similar to uridine, can rescue T cells from DHODH inhibition. Additionally, cancer cells expressing low levels of cytidine deaminase (CDA)—the enzyme converting cytidine to uridine—display increased sensitivity to DHODH inhibitors when extracellular cytidine is abundant. Because CDA is present both intracellularly and in human plasma, these results suggest that reducing extracellular CDA activity could enhance the therapeutic index of DHODH inhibitors, particularly in tumors with inherently low CDA expression.

Materials and Methods

Proteins, sera and chemicals

The chemicals and reagents used in this study were sourced as follows: teriflunomide (Selleck S4169), uridine (Thermo Fisher Scientific # A15227.14), Bay2402234 (Med Chem Express # HY-112645), tetrahydrouridine (Sigma-Aldrich #584223), cytidine (Sigma-Aldrich #C4654), and Brequinar (Biotechne #6196; Sigma, SML0113), recombinant human CDA (Sigma-Aldrich #SRP6372). Inactivated fetal bovine serum was purchased from human serum (whole blood) and Nordic Biolabs (#SV30160.02), was obtained from Sigma-Aldrich (#H6914).

Isolation of primary T cells

Peripheral blood mononuclear cells (PBMCs) were collected from healthy donors and isolated using Ficoll-Paque (GE Healthcare #17-1440-02) density gradient centrifugation. To enrich for T cells, B cells were first removed by depleting them with Dynabeads CD19 Pan B (Invitrogen #11143D), followed by monocyte depletion via plastic adherence.

T cell activation

T cells were stimulated in complete RPMI medium containing 10% serum (either inactivated fetal bovine serum or human serum) and 1% penicillin/streptomycin. Activation was achieved by supplementing the medium with anti-CD3 antibodies (1.25 μg/mL, clone HTT3a, BioLegend #300314) together with anti-CD28 antibodies (2 μg/mL, clone CD28.2, BioLegend #302923).

Monitoring T cell proliferation

Cell divisions were tracked using CFSE (carboxyfluorescein succinimidyl ester, AAT Bioquest #22028) labeling. T cells were resuspended at 1×10^6 cells/mL in PBS containing 5% iFBS and incubated with 5 μM CFSE for 5 minutes at room temperature. Cells were washed twice with PBS, then plated in 96-well plates and subjected to activation and treatment conditions for 48, 72, or 96 hours. Flow cytometric analysis of CFSE dilution was performed on a FACSCalibur (BD Biosciences).

Cell cycle and apoptosis assessment

T cells (1×10^5 per well) were plated in 96-well plates, left either unstimulated or activated, and analyzed for cell cycle progression and apoptosis. For cell cycle analysis, cells were pulsed with 10 μM EdU for 45 minutes and fixed according to the Click-iT™ EdU Alexa Fluor™ 488 Flow Cytometry Assay Kit instructions (Thermo Fisher Scientific #C10425). DNA content was measured after staining with propidium iodide (20 μg/mL) and RNAse (100 μg/mL, Invitrogen #12091) using flow cytometry. Apoptotic cells were detected with the Annexin V-FITC Apoptosis Detection Kit (Abcam #ab14085). Data were analyzed using FlowJo software version 10.2.

Cytotoxicity assay of T cells

To evaluate T cell-mediated killing, activated T cells were co-cultured with 1×10^4 ^{51}Cr-labeled allogeneic lymphoblastoid cells at various effector-to-target ratios in triplicate wells for 4 hours at 37°C with 5% CO2. Following incubation, supernatant radioactivity was measured using a gamma counter (Perkin Elmer),

ensuring that equivalent numbers of viable T cells were applied in each experimental condition.

MTT proliferation assay

T cells were seeded at 1 × 10^5 per well in 200 µL of complete RPMI in 96-well plates and stimulated with anti-CD3/CD28 antibodies under treatment conditions. At specific time points, cells were centrifuged, supernatant discarded, and 100 µL of MTT solution (3 mg/mL in PBS:phenol red-free RPMI, 1:5) was added. Plates were incubated for 3 hours at 37°C, centrifuged again, and frozen at −20°C. After thawing, MTT formazan crystals were solubilized in 25 µL Sorensen's Glycine buffer and 200 µL DMSO, shaken for 10 minutes in the dark, and absorbance was read at 570 nm on a microplate reader (Tecan).

Surface and intracellular staining

T cells (1 × 10^5 per well) were plated and treated according to experimental design. For surface marker analysis, cells were first blocked with Fc block (Invitrogen #L34970) and stained with fixable aqua live/dead dye (BD Pharmingen #564220) for 10 minutes at room temperature. After washing, cells were labeled with antibodies against CD8 (APC, clone HTT8a, BioLegend #300912), CD4 (PE-Cy7, clone OKT4, BioLegend #317414), and CD69 (FITC, clone FN50, BioLegend #310904) for 30 minutes at 4°C. Intracellular detection of IFN-γ (BV421, clone 4S.B3, BioLegend #502532) and granzyme B (Alexa Fluor 647, clone GB11, BioLegend #515406) was carried out using the FoxP3/Transcription Factor Staining Buffer Set (eBioscience #00-5523-00) following manufacturer instructions. Flow cytometric data acquisition was performed on a BD LSR-II instrument, and analysis was conducted with FlowJo v10.2.

Cell lines and culture

Neuroblastoma cell lines (IMR32, SKNBE2, SKNAS, SKNSH, SHSY5Y) were obtained from Marie Arsenian Henriksson's lab, whereas CHP212 and NB1 lines were supplied by Susanne Schlisio's group. SCLC lines (NCIH82, NCIH69) and NSCLC lines (NCIH2030, NCIH358, HCC44) were sourced from ATCC. NCIH82 cells were adapted to adhere in monolayer cultures, except for the spheroid experiments **(Figure 3d).** STR profiling confirmed a 96% match with the original NCIH82 line. Human normal dermal fibroblasts (HNDF) were acquired from PromoCell.

IMR32 cells were maintained in a 1:1 mixture of Nutrient Mixture F12 and Minimum Essential Medium Eagle, supplemented with 10% FBS, 1% penicillin/streptomycin, and 1% non-essential amino acids. SKNBE2, SKNAS, SKNSH, and SHSY5Y were grown in 50% high-glucose DMEM and 50% F12 with 10% FBS and 1% penicillin/streptomycin. CHP212 and NB1 cells were cultured in high-glucose DMEM with 10% FBS and 1% penicillin/streptomycin. All SCLC and NSCLC lines were maintained in RPMI with 10% inactivated FBS and 1% penicillin/streptomycin at 37°C and 5% CO2.

Protein extraction and western blotting

Cells were rinsed twice with PBS before lysis in 150 µL 1× LDS sample buffer (containing Tris-HCl 106 mM, Trisma 141 mM, pH 8.5, 2% LDS, 10% glycerol, 0.51 mM EDTA). Lysates were heated at 95°C for 5 minutes, sonicated in three 10-second bursts, and briefly centrifuged at 16,000 × g. Protein concentrations were quantified using Bio-Rad's DC Protein Assay kit. Equal protein amounts were combined with 4× Laemmli buffer and 100 mM DTT, then heated again at 95°C for 5 minutes.

Samples were separated on 12-well 4–15% TGX stain-free gels at 150 V and activated for 5 minutes using the ChemiDoc Touch system. Proteins were transferred onto PVDF membranes with the Trans-Blot Turbo semidry system (30 min, 25 V, 1 A). Membranes were blocked in 5% milk in PBS-T and incubated overnight with anti-CDA antibody (1 µg/mL). Detection employed HRP-conjugated secondary antibody and Clarity ECL substrate, and total protein loading was verified via stain-free imaging.

CDA detection and functional assays

CDA concentrations in human and mouse samples were quantified using ELISA kits (Cusabio and Aviva, respectively), and enzymatic activity was measured with a BioVision CDA assay kit.

Plasmid-mediated CDA overexpression

A GFP-tagged CDA expression plasmid was transfected into IMR32 and NCIH2030 cells using Lipofectamine 3000. Stably transfected IMR32 cells were selected with G418. NCIH2030 CDA-GFP cells were enriched through G418 selection followed by fluorescence-activated cell sorting for GFP-positive cells.

Live-cell imaging

Cells were plated in 96-well plates at the following densities: 5,000 cells/well for most neuroblastoma lines and HCT116, 3,000–4,000 for NCIH358, 2,000 for NCIH82 and U2OS, 1,500 for HNDF, and 1,000 for NCIH2030 and HCC44. After 24 hours, 0.3 µM YOYO-3 dye was added to monitor dead cells. Plates were incubated in an IncuCyte S3 system within a CO2 incubator, and images were acquired every 2 hours. Confluency and YOYO-3-positive cells were analyzed with the IncuCyte software, normalizing cell death to confluency. Data were graphed using GraphPad Prism v8 as mean ± SEM from at least three independent experiments.

Spheroid formation assay

NCIH82 cells cultured in suspension were collected by centrifugation at 1,200 × g for 5 minutes. After removing the supernatant, the pellet was resuspended in 1 mL of complete RPMI medium containing inactivated fetal bovine serum (iFBS). Viable cells were enumerated and adjusted to a density of 12,500 cells per mL. For spheroid formation, 80 µL of the cell suspension was added to each well of a 96-well ultra-low attachment plate (Costar #7007). Microscopic inspection ensured that single cells aggregated appropriately; gentle tapping was applied to promote clustering when necessary. Cultures were incubated at 37°C for 48 hours. On day 2, 100 µL of fresh medium was added carefully to each well. By day 5, spheroids were fully formed, at which point the medium was replaced with 100 µL of fresh complete RPMI containing the experimental compounds, resulting in a total volume of 200 µL per well. Apoptotic activity was monitored by adding 0.375 µM caspase 3/7 reagent (Invitrogen #C10423). Plates were imaged at 4-hour intervals using the IncuCyte S3 system in a CO2-controlled incubator, following an initial 30-minute stabilization period.

Statistical procedures

Each experimental condition included 3–4 technical replicates. Statistical analyses were conducted in GraphPad Prism v8.4.3, with significance thresholds defined as: *P* values: * < 0.05, ** < 0.01, *** < 0.001, **** < 0.0001.

Gene expression data from 1,389 cell lines in the Cancer Cell Line Encyclopedia (CCLE, 21q4) were extracted using the Datagrabber tool on the R2 platform (https://hgserver1.amc.nl/cgi-bin/r2/main.cgi). Microarray expression profiles of tumors (MAS5.0 normalized) were retrieved through the MegaSampler tool on R2. Comparisons between groups were performed using Welch's T-test and the Mann-Whitney U test as appropriate. To control for multiple comparisons, the Benjamini-Hochberg method was applied using the Statsmodels package.

Results and Discussion

Cytidine protects activated T cells from DHODH inhibition

We first evaluated the effects of DHODH inhibitors (DHODHi) on T cells from healthy donors cultured in medium containing inactivated fetal bovine serum (iFBS) **(Figure 1a).** As expected, activated T cells were highly sensitive to DHODHi, showing pronounced inhibition of proliferation. By contrast, quiescent T cells were largely unaffected by the inhibitors and were able to proliferate normally after DHODHi removal and subsequent activation **(Figure 1b).**

Exposure of activated T cells to DHODHi resulted in increased cell death and a reduction in the fraction of cells entering S-phase. Supplementing the culture medium with excess uridine rescued these cells, consistent with activation of the pyrimidine salvage pathway **(Figures 1c and 1d).** Notably, T cells that survived brequinar treatment exhibited only partially preserved cytotoxic activity **(Figure 1e),** despite unchanged expression of the early activation marker CD69. In contrast, resting T cells maintained full cytotoxic potential following inhibitor withdrawal and later activation **(Figure 1f)**.

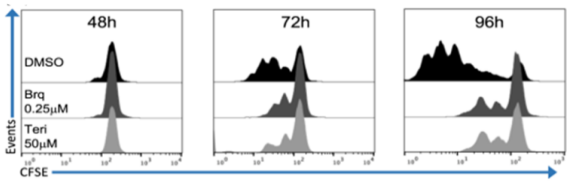

a)

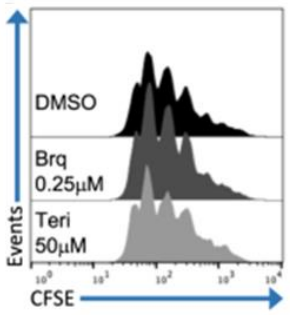

b)

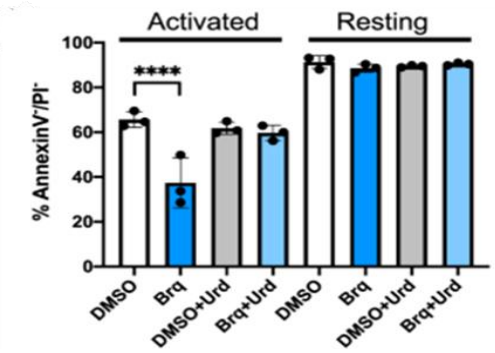

c)

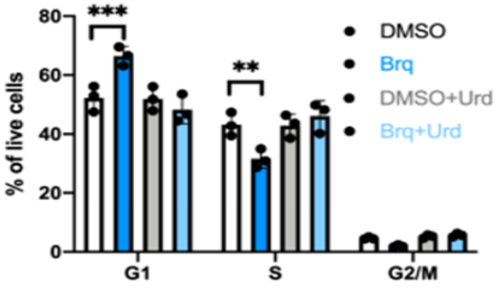

d)

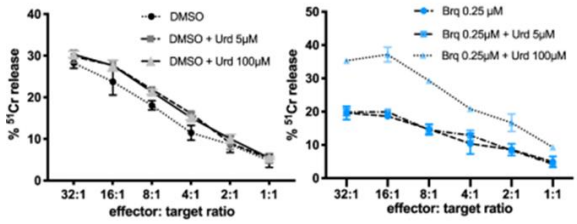

e)

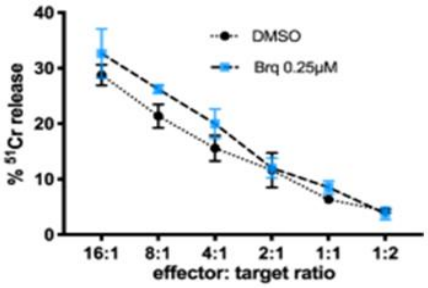

f)

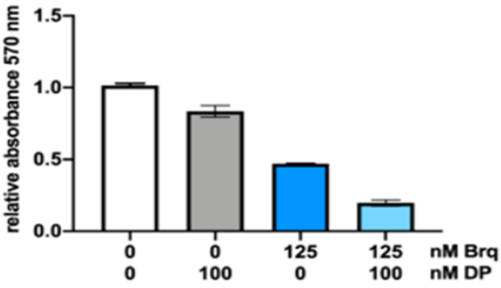

g)

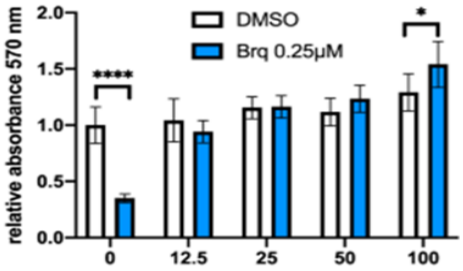

h)

Figure 1. cytidine protects activated t cells from DHODH inhibition

To begin, we confirmed the well-known antiproliferative effect of DHODH inhibitors (DHODHi) on activated human T cells cultured in medium containing inactivated fetal bovine serum (iFBS) **(Figure 1a).** Activated T cells exhibited strong growth suppression when treated with brequinar or teriflunomide for 48, 72, or 96 hours following activation with anti-CD3/CD28 antibodies, as assessed by CFSE dilution and flow cytometry. In contrast, quiescent T cells were largely resistant to DHODHi and regained normal proliferative capacity after the inhibitors were removed and the cells subsequently activated **(Figure 1b).**

DHODH inhibition in activated T cells led to increased apoptosis and a marked decrease in S-phase entry. These effects were reversed by supplementing the medium with excess uridine, indicating engagement of the pyrimidine salvage pathway **(Figures 1c and 1d).** Notably, surviving T cells displayed only partial preservation of cytotoxic activity following brequinar treatment **(Figure 1e)**, despite unaltered expression of the early activation marker CD69. Resting T cells, however, maintained full cytotoxic function once the DHODHi was removed and the cells were subsequently activated **(Figure 1f)**.

Activated T cells rely heavily on pyrimidine ribonucleotide synthesis, requiring an approximately eightfold expansion of nucleotide pools [15]. Reflecting

this metabolic demand, mRNA expression of enzymes involved in pyrimidine metabolism rapidly changes upon T cell activation. For instance, within 4 hours of activation, human T cells upregulate transcripts for the nucleoside transporter SLC29A1 and the uridine/cytidine kinase UCK2 [16], and increases in some of these proteins have been confirmed at the protein level [17-19]. Human plasma uridine concentrations are in the low micromolar range and fluctuate throughout the day [20]. Since cellular uridine uptake can reduce DHODHi efficacy [21], blocking nucleoside transporters with agents such as dipyridamole, which inhibits SLC29A1, has been proposed to enhance the antitumor activity of DHODH inhibitors [22-24]. We evaluated this approach in activated T cells and found that dipyridamole alone had minimal impact, but it potentiated the growth-inhibitory effects of brequinar **(Figure 1g).** These results suggest that, when combining DHODHi with nucleoside transport inhibitors in a clinical setting, potential adverse effects on T cell function should be carefully considered. Previous studies reported that millimolar concentrations of deoxycytidine could rescue K562 leukemia cells from DHODH inhibition [25]. However, this approach did not rescue activated human T cells and addition of thymidine, alone or with deoxycytidine, was also ineffective. In contrast, supplementing the culture medium with cytidine efficiently rescued activated T cells from DHODH inhibition **(Figure 1h),** indicating that these cells can utilize cytidine via the salvage pathway. These findings suggest that increasing extracellular cytidine could be a strategy to protect T cells during DHODHi treatment.

Solid tumors with low CDA expression

To identify cancers potentially hypersensitive to DHODH inhibition, we analyzed mRNA levels of pyrimidine salvage pathway enzymes using the DepMap portal (https://depmap.org/portal/interactive/). This analysis revealed consistently low expression of cytidine deaminase (CDA) in several tumor types, including cell lines derived from pediatric cancers such as neuroblastoma **(Figure 2a).** CDADC1 is another enzyme with cytidine deaminase activity, but its expression did not vary significantly across most tumor types except chondrosarcomas (https://depmap.org/portal/interactive/).

To validate these findings, we examined CDA expression in the Cancer Cell Line Encyclopedia (CCLE) 21q4 dataset via R2 (http://r2.amc.nl) and found that CDA expression was significantly lower (FDR < 0.01) in certain pediatric cancers, including neuroblastoma (two-sided Welch's t-test, FDR < 1×10^{-35}). These observations suggest that tumors with low CDA expression may be particularly vulnerable to DHODH inhibition, especially in conditions where extracellular cytidine is abundant.

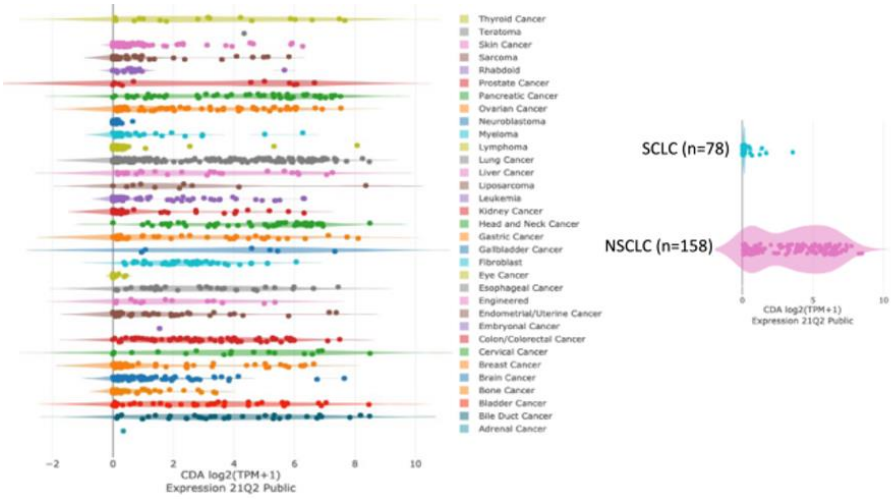

a)

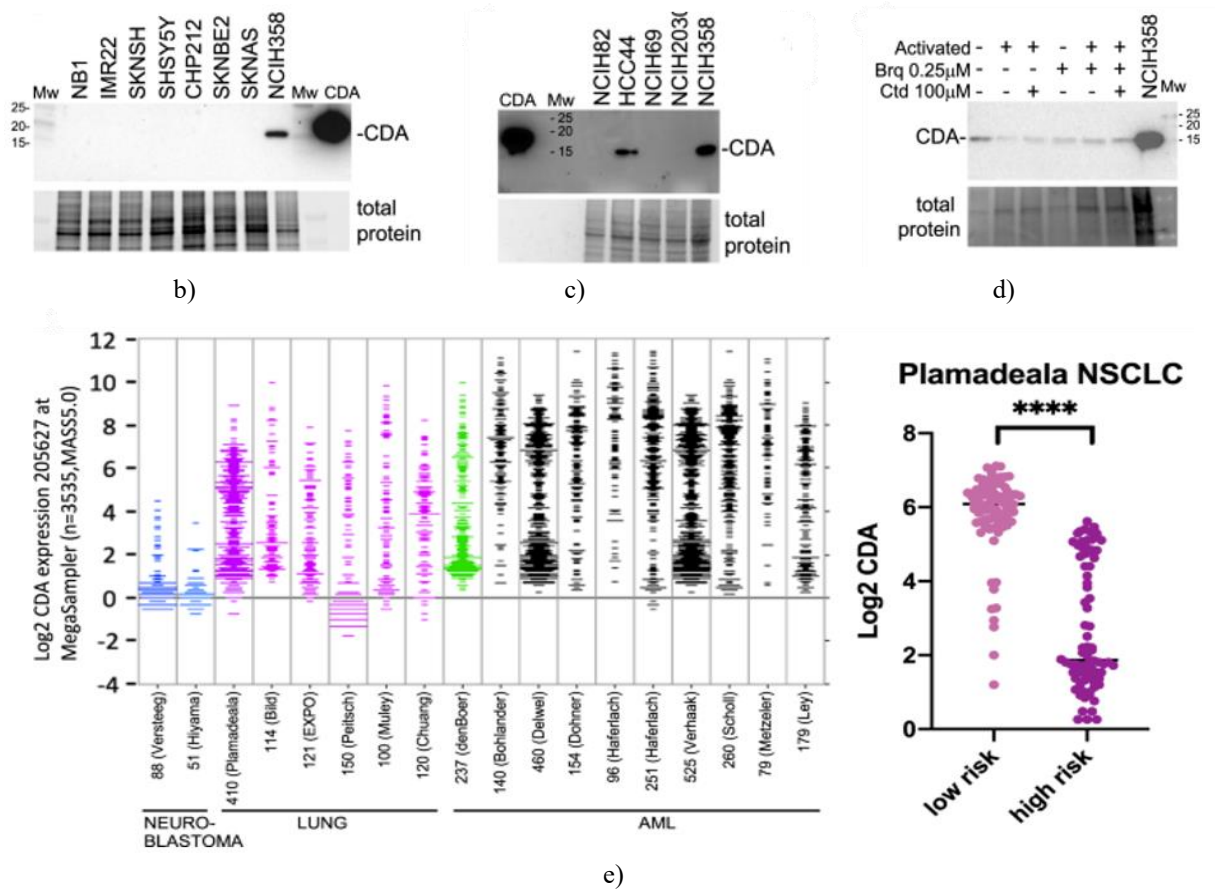

Figure 2. Identification of cancers with altered pyrimidine nucleotide metabolism enzyme expression

Analysis of CDA mRNA in various cancer cell lines using the DepMap portal revealed consistently low expression in several tumor types, including small cell lung carcinoma (SCLC) and neuroblastoma **(Figure 2a).** CDA protein levels were confirmed by Western blot in neuroblastoma **(Figure 2b)** and lung cancer cell lines **(Figure 2c)**. Similarly, CDA protein was detectable in both resting and 48-hour activated T cells under the indicated conditions **(Figure 2d).** Examination of tumor samples from the R2 Genomics Analysis and Visualization Platform showed that neuroblastoma consistently exhibits low CDA expression, whereas lung cancer and AML display more variable levels **(Figure 2e).** In one lung cancer dataset (Plamadeala study), high-risk NSCLC tumors were associated with lower CDA expression, while pediatric AML frequently exhibited low CDA expression (denBoer study).

CDA and several other genes involved in uracil and cytosine nucleotide metabolism are located on chromosome 1p, a region often deleted in neuroblastoma [26]. However, CDA mRNA expression did not appear to correlate with 1p status: all tested neuroblastoma cell lines showed low CDA levels regardless of deletion status. For example, the mean CDA expression in cell lines with 1p deletion (log2[TPM] = 0.086) was lower than in lines without deletion (log2[TPM] = 0.170), but this difference was not statistically significant (Mann-Whitney U test, two-sided, p = 0.179). The 1p locus also contains genes crucial for cell survival and proliferation beyond those involved in pyrimidine metabolism. Consistent with mRNA data, Western blot analysis revealed undetectable CDA protein in all neuroblastoma cell lines examined **(Figure 2b).**

SCLC cell lines similarly showed low CDA mRNA expression **(Figure 2a),** confirmed by the absence of protein detection in NCIH69 and NCIH82 cells **(Figure 2c).** Analysis of CCLE data further indicated significantly reduced CDA expression in SCLC (FDR < 0.01; two-sided Welch's t-test, FDR < 1 × 10^−35, aligning with previous reports that SCLC is particularly sensitive to DHODH inhibition [9]. In contrast, non-small cell lung carcinoma (NSCLC) cell lines generally

exhibited higher CDA expression, though with considerable variability **(Figure 2a).** For instance, NCIH2030 cells expressed low CDA, while NCIH358 and HCC44 expressed higher levels **(Figure 2c)**.

In T cells, CDA mRNA is very low [16], but protein is detectable in both resting and activated CD4+ and CD8+ T cells [17]. Consistently, Western blot analysis confirmed CDA expression in resting and activated T cells **(Figure 2d).**

Excess cytidine sensitizes low-CDA cancer cells to DHODH inhibition

These findings suggested that cancer cells and T cells may respond differently to DHODHi, particularly in media supplemented with cytidine. Consistent with expectations, uridine supplementation protected IMR32 neuroblastoma cells from brequinar **(Figure 3a).** However, unlike activated T cells, cytidine did not confer protection to IMR32 cells. Instead, in the presence of brequinar, cytidine increased cytotoxicity and rapidly inhibited proliferation **(Figure 3a)**. Experiments using identical seeding densities confirmed the differential response between T cells and IMR32 cells.

Additional testing across other neuroblastoma cell lines revealed that IMR32 and SHSY5Y were most sensitive to the combined brequinar+cytidine treatment, showing immediate and pronounced growth inhibition. SKNSH and CHP212 cells also displayed increased cell death, whereas SKNBE2 and SKNAS cells were less affected; both express mutant p53, which is uncommon in neuroblastoma and may influence DHODHi sensitivity, as DHODH inhibitors are known to activate p53 [2]. NB1 cells were highly sensitive to brequinar alone, and cytidine supplementation did not further enhance this effect. NB1 cells are notable for a high mutational burden (963 mutations), single copies of TP53 and CDKN1A, an extra copy of CDADC1, and ALK amplification—unique among the tested neuroblastoma lines (https://depmap.org/portal/interactive).

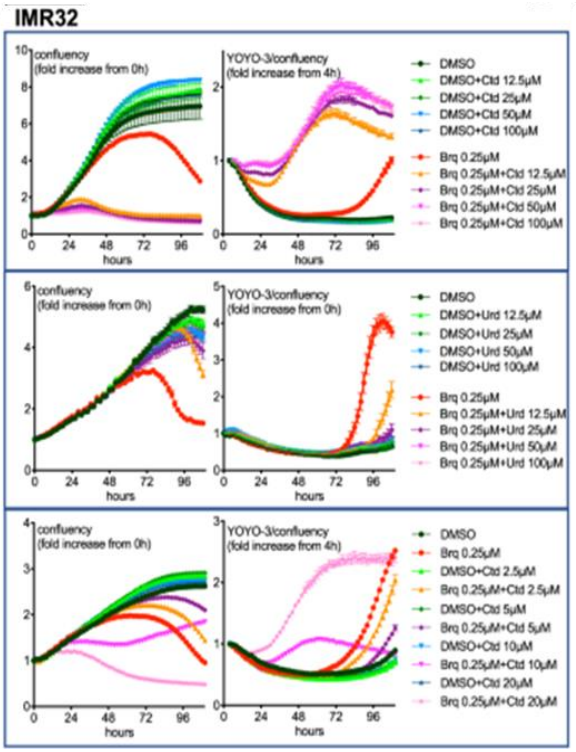

a)

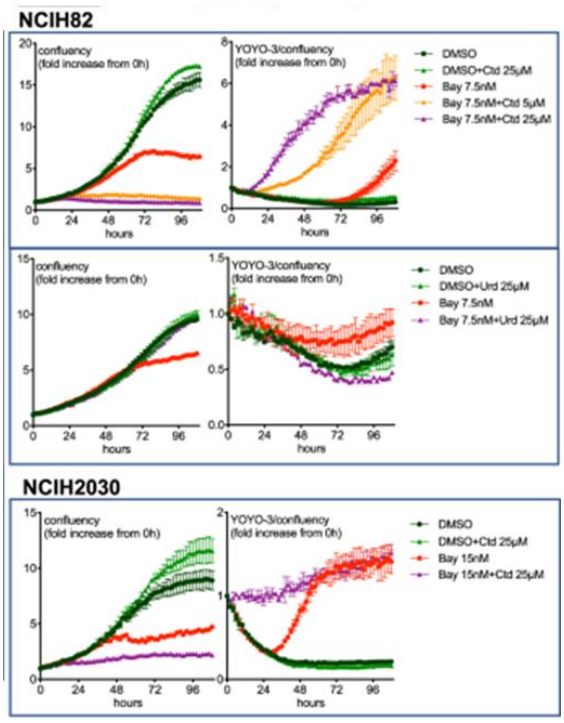

b)

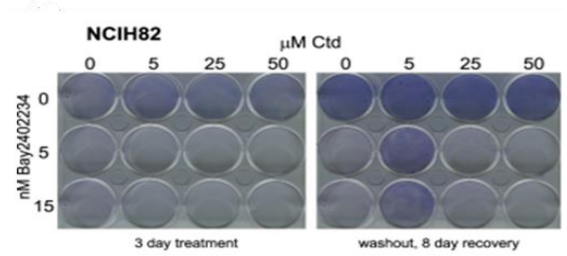

c)

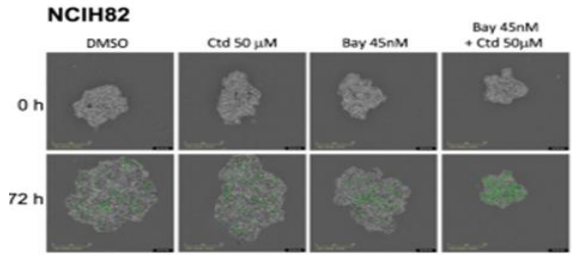

d)

Figure 3. Cytidine Supplementation Sensitizes Low-CDA Cancer Cells to DHODH Inhibitors

NCIH2030 (NSCLC), IMR32 (neuroblastoma), and NCIH82 (SCLC) cells were treated as indicated, and cell proliferation and death were monitored using the IncuCyte system by measuring confluency and YOYO-3 red staining normalized to confluency (Materials and Methods) **(Figures 3a and 3b).** Clonogenic assays with NCIH82 cells demonstrated that the combination of Bay2402234 and cytidine strongly reduced colony formation **(Figure 3c)**. Additionally, NCIH82 cells grown as spheroids exhibited pronounced caspase-3/7 activation when treated with the same combination **(Figure 3d**), (green signal).

Intracellular CDA confers protection against DHODHi and cytidine

To determine whether the cytotoxicity of the DHODHi+cytidine combination observed in iFBS-grown neuroblastoma cells was generalizable to other cancers, we tested lung cancer cell lines with varying CDA expression. Low-CDA NCIH82 (SCLC) and NCIH2030 (NSCLC) cells showed enhanced sensitivity to cytidine combined with Bay2402234, a potent and selective DHODH inhibitor [8] **(Figures 3b and 3c).** Although both cell lines lack functional p53, NCIH82 harbors RB1 mutations and exhibits a 24-fold increase in c-Myc mRNA compared to normal cells (https://depmap.org/portal/interactive), whereas NCIH2030 carries oncogenic KRas, a feature previously linked to DHODHi susceptibility [27, 28]. Notably, the DHODHi+cytidine combination also induced strong cytotoxicity in NCIH82 spheroids **(Figure 3d).**

Conversely, NSCLC lines with high CDA expression, such as HCC44 and NCIH358, were effectively rescued from DHODHi-induced growth inhibition by cytidine **(Figures 4a and 4b).** If the protective effect of cytidine depends on CDA activity, inhibition of CDA with the small molecule tetrahydrouridine (THU) should abolish this rescue. Indeed, treatment with THU prevented cytidine-mediated protection against DHODHi in high-CDA cancer cells **(Figure 4a)**. Similarly, overexpression of CDA in low-CDA cell lines reduced the cytotoxicity of the DHODHi+cytidine combination **(Figures 4c–4e).** Importantly, human normal dermal fibroblasts were resistant to all treatments over at least a 4.5-day observation period.

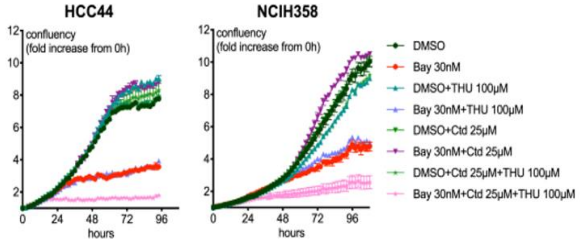

a)

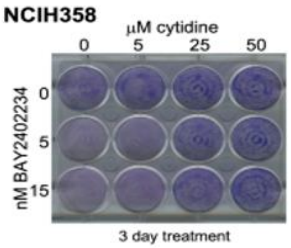

b)

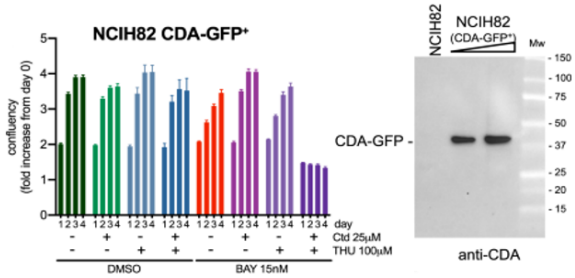

c)

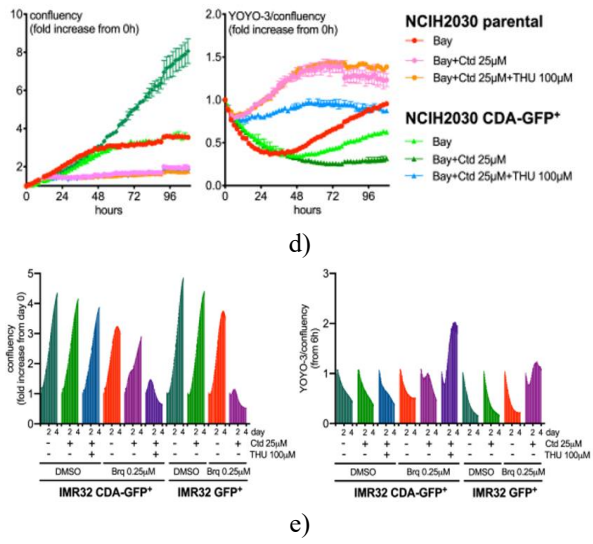

Figure 4. Role of Intracellular CDA in Modulating Sensitivity to DHODH Inhibitors and Cytidine

We next examined the influence of CDA on the response of NSCLC cells to DHODH inhibition in the presence of cytidine. HCC44 and NCIH358 cells were treated under the indicated conditions, and proliferation was tracked using the IncuCyte platform **(Figure 4a).** Consistent results were obtained in clonogenic assays with NCIH358, where the Bay2402234 and cytidine combination markedly reduced colony formation **(Figure 4b).**

To directly test the protective role of CDA, low-CDA cell lines (IMR32, NCIH2030, and NCIH82) were engineered to overexpress CDA fused to GFP. In these cells, CDA-GFP expression substantially alleviated the growth-inhibitory effect of DHODHi plus cytidine **(Figures 4c–4e),** and Western blotting confirmed the successful expression of the fusion protein.

Interestingly, partial cytidine-mediated rescue was observed in low-CDA cells at submaximal concentrations of cytidine **(Figures 3a and 3c)**, suggesting that maintaining sufficiently high extracellular cytidine in vivo would be necessary for therapeutic benefit (Discussion).

Effect of human serum on DHODHi sensitivity

All previous experiments were performed using standard culture medium supplemented with inactivated fetal bovine serum (iFBS). To better approximate physiological conditions, we repeated key experiments with medium containing human serum (HS).

Under these conditions, IMR32, NCIH82, and NCIH2030 cells displayed increased sensitivity to DHODHi alone compared with iFBS-supplemented cultures **(Figures 3 and 5).** This observation may reflect lower uridine levels in human serum relative to FBS. Supporting this notion, enzymes responsible for uridine catabolism (DPYD, DPYS, UPB1) are present in human plasma (https://www.proteinatlas.org/). Indeed, supplementation with uridine rescued IMR32 and NCIH82 cells from DHODHi-induced growth inhibition in HS. It is important to note, however, that this heightened sensitivity observed in vitro is unlikely to occur in vivo, where circulating uridine concentrations are tightly controlled at approximately 3–5 μM [20].

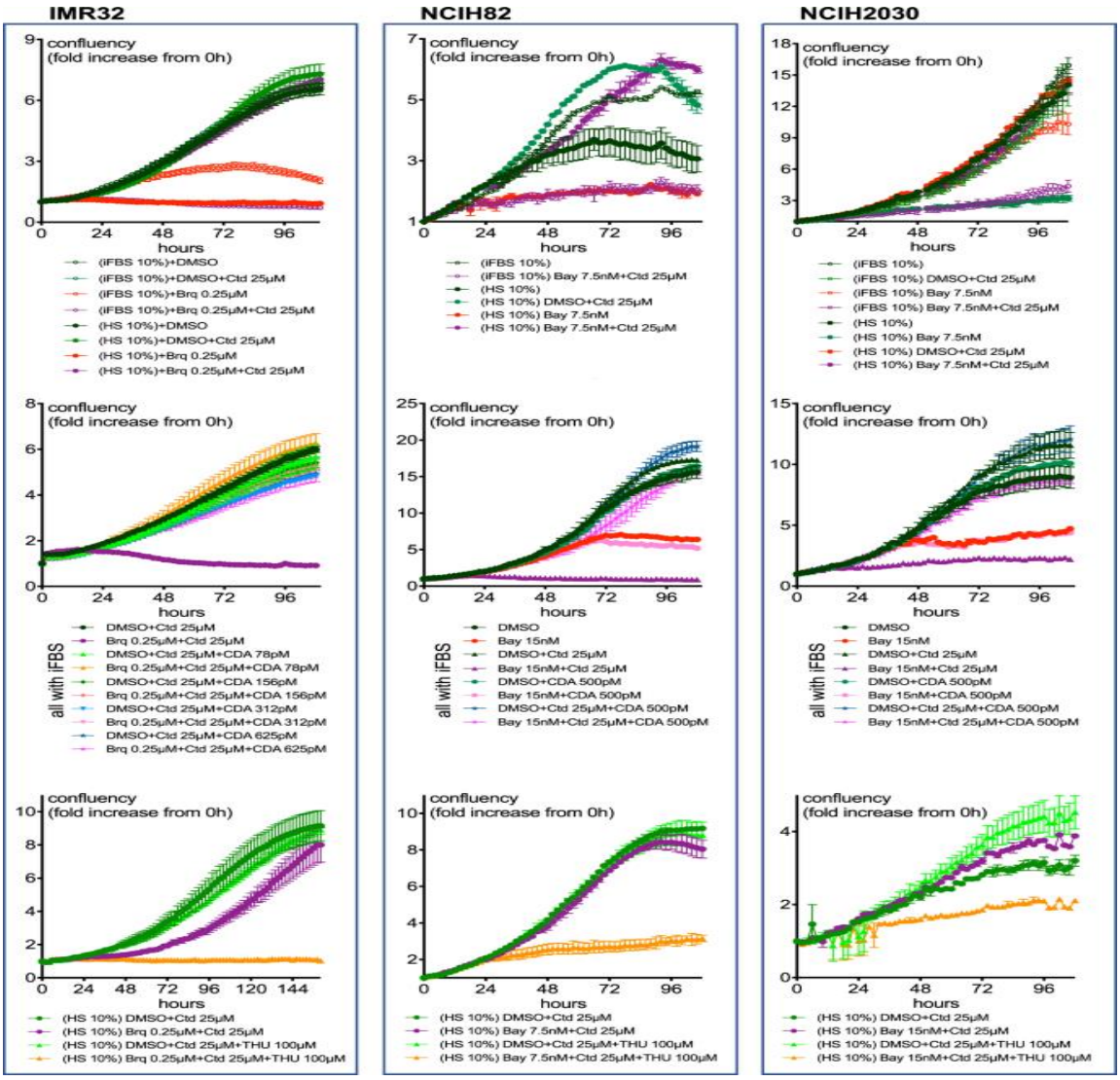

Figure 5. Human serum modulates the response of Low-CDA cancer cells to DHODH inhibitors and cytidine

IMR32, NCIH82, and NCIH2030 cells were cultured in medium supplemented with either FBS or human serum (HS) and treated with the indicated compounds or recombinant human CDA. Cell proliferation was monitored using the IncuCyte system.

A striking difference emerged between cells grown in iFBS versus HS: low-CDA cancer cells in HS were effectively rescued by 25 μM cytidine **(Figure 5)**, whereas the same treatment in iFBS proved highly cytotoxic **(Figure 3)**. This difference is likely attributable to the presence of cytidine deaminase activity and CDA protein in human serum/plasma [29, 30] (https://www.proteinatlas.org/), which can efficiently convert cytidine to uridine. Supporting this notion, supplementation with recombinant CDA in iFBS cultures restored cell viability under DHODHi+cytidine treatment **(Figure 5)**. Conversely, inhibition of CDA using tetrahydrouridine prevented proliferation of IMR32, NCIH82, and NCIH2030 cells in HS under the same treatment conditions **(Figure 5).**

Interestingly, cytidine concentrations above 25 μM were less effective at rescuing IMR32 cells in HS from brequinar-induced toxicity, suggesting that the endogenous CDA in 10% HS is insufficient to process large cytidine excess. Addition of recombinant CDA restored protection even at these higher cytidine levels. It is also worth noting that while FBS experiments were conducted with inactivated serum, HS experiments used non-inactivated serum; serum inactivation did not qualitatively alter the results.

Activated T cells retain cytotoxic function under DHODHi+cytidine treatment

Although low-CDA cancer cells in HS were highly sensitive to DHODHi alone, this sensitivity is unlikely to fully reflect in vivo conditions due to circulating uridine concentrations of 3–5 µM. Moreover, DHODHi strongly impaired activated T cell proliferation in HS **(Figure 6a),** highlighting the need to protect immune cells during treatment. Supplementation with cytidine effectively rescued activated T cells from brequinar-induced growth inhibition in HS, similar to observations in iFBS cultures **(Figures 1h and 6a).**

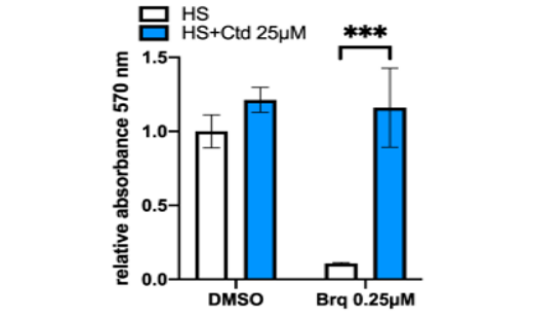

a)

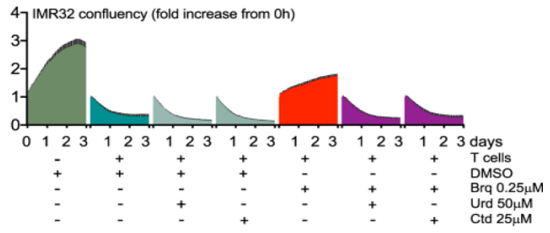

b)

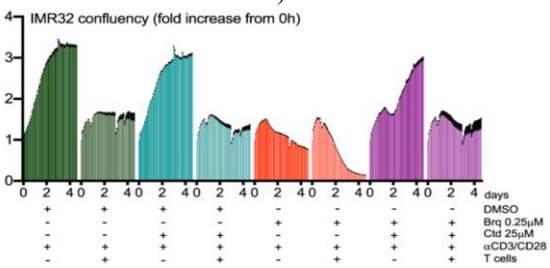

c)

Figure 6. Preservation of T cell cytotoxicity in human serum

(a) Human T cells were cultured in medium containing human serum (HS) and treated with the indicated compounds during activation. Cellular proliferation was quantified using an MTT assay. Data represent the average of three independent technical replicates, with error bars indicating standard deviation (SD). Statistical significance was assessed by two-way ANOVA. (b) T cells were activated for three days in HS medium with DMSO or brequinar, either alone or combined with cytidine or uridine. Following activation, T cells were washed, and a fixed number of 80,000 viable cells were transferred to GFP-labeled IMR32 cultures maintained in compound-free HS medium. GFP intensity was continuously monitored using the IncuCyte system. All conditions were performed in triplicate; SEM is shown as error bars. (c) To further evaluate T cell-mediated killing, resting T cells were added to GFP-labeled IMR32 cells in HS-containing medium and then activated in situ with anti-CD3/CD28 antibodies in the presence or absence of brequinar and/or cytidine. Growth of GFP-positive cancer cells was tracked over time with the IncuCyte system. Experiments were performed in triplicate with SEM indicated in black. These experiments revealed that T cells activated in HS could eliminate IMR32 cells effectively. However, activation in the presence of brequinar alone partially reduced T cell cytotoxicity. Supplementation with cytidine or uridine during activation restored T cell-mediated killing, counteracting the inhibitory effects of brequinar (b). In co-culture experiments where T cells were activated after being added to cancer cells (c), they maintained their ability to eradicate the tumor cells even with brequinar+cytidine treatment, although cytidine slightly enhanced IMR32 growth, highlighting a context-dependent protective effect.

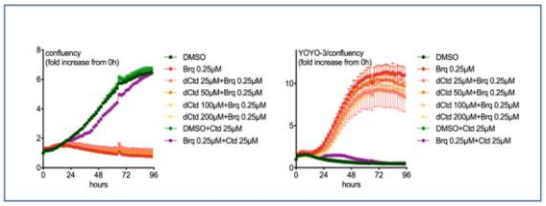

a)

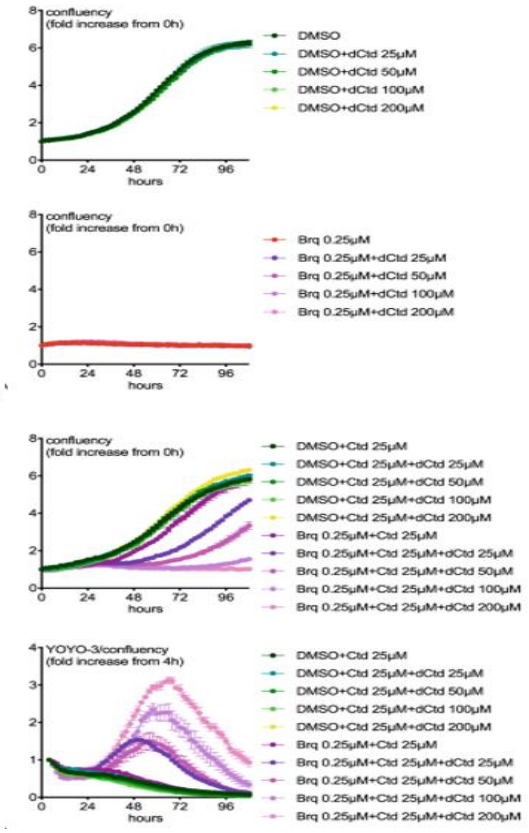

b)

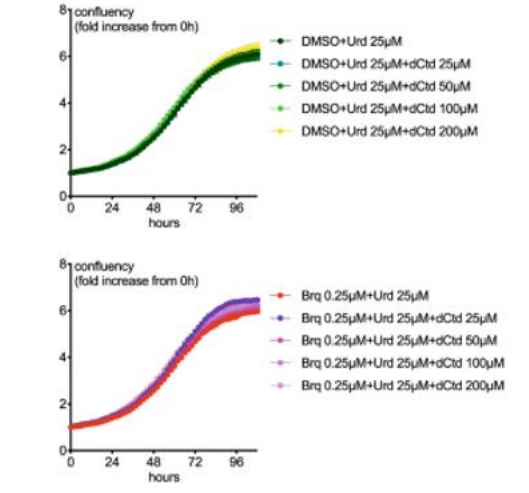

c)

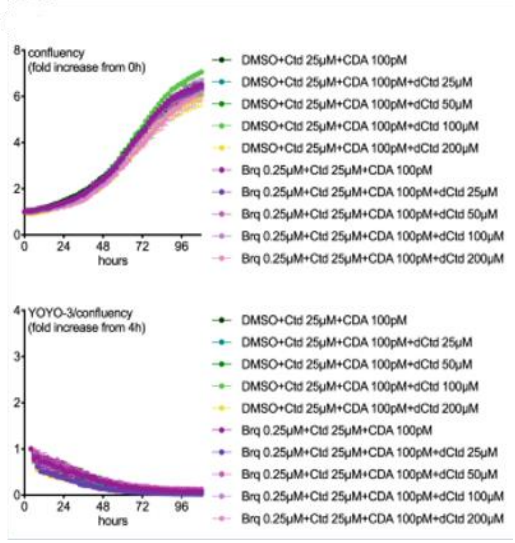

d)

Figure 7. Impact of deoxycytidine on IMR32 neuroblastoma cells in the context of DHODH Inhibition and cytidine supplementation

(a–d) IMR32 cells were cultured in human serum (HS)-supplemented medium and treated with brequinar alone or in combination with cytidine, in the presence or absence of deoxycytidine or recombinant human CDA. Cell proliferation and viability were continuously monitored using the IncuCyte system. Data presented in panels b–d were derived from the same experimental setup.

Deoxycytidine does not impair t cell-mediated killing of IMR32 cells

As previously observed in iFBS-supplemented medium, deoxycytidine does not confer protection to activated T cells from DHODH inhibition. **Figure 8a** demonstrates that this also holds true when T cells are cultured in HS. Moreover, unlike its effect on IMR32 cells, deoxycytidine does not interfere with cytidine-mediated rescue of T cells, indicating that deoxycytidine selectively modulates cytidine effects in cancer cells without impairing T cell function.

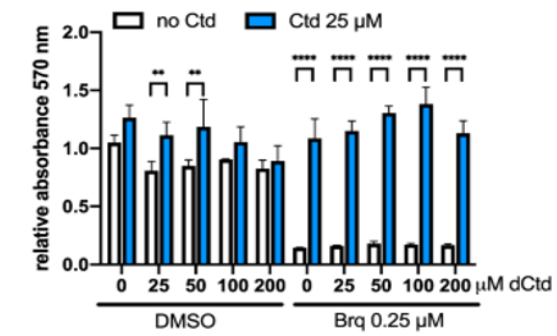

a)

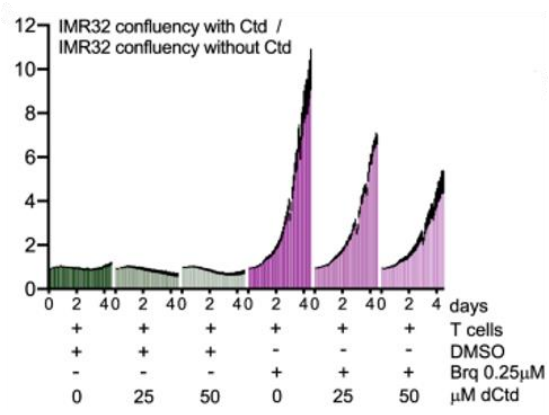

b)

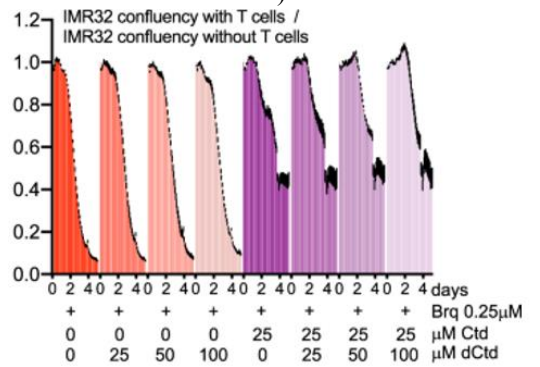

c)

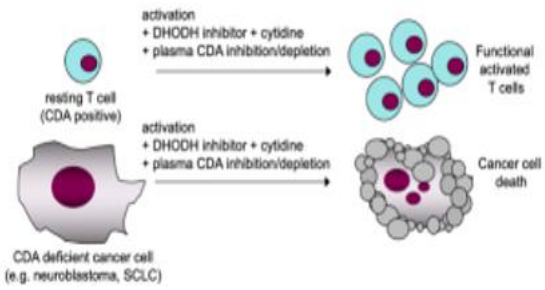

d)

Figure 8. Deoxycytidine does not impair t cell cytotoxicity against IMR32 cells

(a) Activated human T cells were cultured in medium containing human serum (HS) with the indicated treatments, and their proliferation was evaluated after four days using an MTT assay. Data represent the mean of three independent technical replicates, with standard deviation (SD) indicated by error bars. Statistical comparisons were performed using two-way ANOVA. (b) To examine T cell-mediated cytotoxicity in a co-culture system, 100,000 T cells were added to 40,000 GFP-labeled IMR32 cells. T cells were stimulated with anti-CD3/CD28 antibodies in the presence of brequinar and/or nucleosides. Cancer cell growth was tracked using the IncuCyte system, and the ratio of GFP-positive cell confluency with and without 25 µM cytidine was calculated. Experiments were done in triplicate, with SEM shown. (c) A complementary experiment assessed T cell killing in the presence of brequinar (0.25 µM) with or without 100,000 T cells, all samples receiving anti-CD3/CD28 stimulation. The impact of T cells on IMR32 proliferation was quantified by comparing GFP-positive cell confluency between wells with and without T cells. Triplicate measurements were collected, with SEM indicated. (d) Proposed Model

Mouse plasma contains higher cytidine concentrations than human plasma, and CDA was undetectable in mouse serum using the available reagents, making mouse models unsuitable for directly studying the effects of plasma CDA depletion. To overcome this, we utilized co-cultures of human T cells and cancer cells in HS medium. In this setting, deoxycytidine partially blocked the cytidine-mediated protection of IMR32 cells **(Figure 8b).** Crucially, deoxycytidine did not compromise the cytotoxic function of T cells against IMR32 cells treated with brequinar **(Figure 8c)**, demonstrating that deoxycytidine selectively affects cancer cell rescue without impairing T cell activity.

This study demonstrates that extracellular cytidine can safeguard activated T cells against the effects of DHODH inhibitors, suggesting that increasing plasma cytidine levels in humans might mitigate the immunosuppressive impact of these compounds. Our findings also indicate that tumors expressing low levels of cytidine deaminase (CDA) are particularly vulnerable to DHODH inhibition, especially under conditions where cytidine is abundant. As illustrated in **Figure 2**, several cancer cell lines consistently exhibit low CDA expression, with a significant fraction across various tumor types showing

poor enzyme levels. Notably, most neuroblastoma and small cell lung carcinoma (SCLC) cell lines fall into this category, and encouraging preclinical results have been reported in murine models of these cancers [6, 9]. In contrast, acute myeloid leukemia (AML) generally does not display consistently low CDA expression, except for some childhood AML cases according to available datasets **(Figure 2e).** Since clinical trials have predominantly focused on adult AML patients, these findings underscore the potential of increasing plasma cytidine to enhance the therapeutic index of DHODH inhibitors in patients with CDA-deficient tumors (see working model) **(Figure 8d).**

A critical question arising from these observations is whether plasma cytidine can be raised to therapeutically relevant levels. Dietary cytidine is likely rapidly converted to uridine in the gastrointestinal tract and liver [31], implying that systemic administration via injection or possibly oral delivery as CDP-choline [32] may be required. Unlike uridine, cytidine is not metabolized by mammals unless converted into uridine, increasing the likelihood of achieving elevated plasma concentrations. In mice, a single intraperitoneal injection of cytidine at 3500 mg/kg produced peak plasma levels around 10 mM within one hour, which were largely maintained for at least four hours. During this period, cytidine was partially deaminated to uridine, but uridine levels did not exceed cytidine concentrations [33]. It is also important to note that pyrimidine nucleoside administration may influence body temperature [20, 33-35]; however, unlike uridine, cytidine injections in rabbits did not alter body temperature [34].

Reducing or inhibiting plasma CDA activity could further aid in maintaining high cytidine levels. Cell-permeable CDA inhibitors, such as tetrahydrouridine (THU), are under investigation in combination with approved cytidine analogues like decitabine, which are otherwise inactivated by CDA [36, 37]. Nevertheless, these inhibitors may also affect intracellular CDA in normal cells, including T cells, potentially diminishing antitumor immunity. By contrast, deoxycytidine appears to act by competing with cytidine for plasma CDA, without adversely affecting T cell function, as shown in our studies. These observations serve primarily as proof-of-concept, highlighting the need to develop strategies for selectively inhibiting or removing plasma CDA—potentially through non-cell-permeable inhibitors or plasmapheresis/immunoadsorption systems [38]—since deoxycytidine is likely to be rapidly taken up or cleared in vivo. Such approaches could be immediately valuable for patients unresponsive to cytidine analogues and may also enhance the therapeutic index of DHODH inhibitors. Evidence suggests that plasma CDA originates largely from neutrophils, which express high levels of the enzyme (https://www.proteinatlas.org/). Neutrophils are short-lived, infiltrate many tumor types, and account for approximately 70% of human white blood cells and 20–30% in mice, with this proportion increasing with age [36, 39–46]. This implies that CDA may accumulate in plasma over time in response to various stressors. Indeed, elevated circulating CDA has been observed in conditions such as sepsis, metastatic cancer, rheumatoid arthritis, and systemic lupus erythematosus [36, 39–42, 47, 48]. While plasma uridine levels remain largely stable, cytidine concentrations may be lower in adults compared with infants [13].

Conclusion

Consequently, infants or adult patients with low plasma CDA, particularly those whose tumors also lack CDA expression, may respond more favorably to DHODH inhibition while experiencing reduced side effects such as immunosuppression. Collectively, these findings suggest that targeting extracellular CDA—and possibly other plasma-accumulated enzymes—represents a promising strategy to improve cancer therapy outcomes.

Acknowledgments: This work was supported by a Cancerfonden grant (project 190096) a Barncancerfonden grant (PR2019-0089), a Radiumhemmet grant (project 191172) and a Vetenskapsrådet grant (project 2017-02041). O.B.R. was supported by grants from Barncancerfonden (TJ2021-0137 and PR2021-0129) and the KI Network Medicine Global Alliance. We thank Saikiran Sedimbi for technical assistance.

Conflict of Interest: None

Financial Support: Open access funding provided by Karolinska Institute.

Ethics Statement: None

References

1. Mollick T, Laín S. Modulating pyrimidine ribonucleotide levels for the treatment of cancer. Cancer Metab. 2020;8:12.
2. Ladds MJGW, van Leeuwen IMM, Drummond CJ, Chu S, Healy AR, Popova G, et al. A DHODH inhibitor increases p53 synthesis and enhances tumor cell killing by p53 degradation blockage. Nat Commun. 2018;9:1107.
3. Ladds MJGW, Popova G, Pastor-Fernández A, Kannan S, van Leeuwen IMM, Håkansson M, et al. Exploitation of dihydroorotate dehydrogenase (DHODH) and p53 activation as therapeutic targets: a case study in polypharmacology. J Biol Chem. 2020;295:17935–17949.
4. Popova G, Ladds MJGW, Johansson L, Saleh A, Larsson J, Sandberg L, et al. Optimization of tetrahydroindazoles as inhibitors of human dihydroorotate dehydrogenase and evaluation of their activity and in vitro metabolic stability. J Med Chem. 2020;63:3915–3934.
5. Zhou Y, Tao L, Zhou X, Zuo Z, Gong J, Liu X, et al. DHODH and cancer: promising prospects to be explored. Cancer Metab. 2021;9:22.
6. Olsen TK, Dyberg C, Embaie B, Alchahin A, Milosevic J, Otte J, et al. DHODH is an independent prognostic marker andpotent therapeutic target in neuroblastoma. JCI Insight. 2022;7:e153836.
7. Sykes DB, Kfoury YS, Mercier FE, Wawer MJ, Law JM, Haynes MK, et al. Inhibition of dihydroorotate dehydrogenase overcomes differentiation blockade in acute myeloid leukemia. Cell. 2016;167:171–186.e15.
8. Christian S, Merz C, Evans L, Gradl S, Seidel H, Friberg A, et al. The novel dihydroorotate dehydrogenase (DHODH) inhibitor BAY 2402234 triggers differentiation and is effective in the treatment of myeloid malignancies. Leukemia. 2019;33:2403–2415.
9. Li L, Ng SR, Colón CI, Drapkin BJ, Hsu PP, Li Z, et al. Identification of DHODH as a therapeutic target in small cell lung cancer. Sci Transl Med. 2019;11:eaaw7852.
10. Moyer, JD, Oliver, JT & Handschumacher, RE. Salvage of circulating pyrimidine nucleosides in the rat. Cancer Res. 1981;41: 9.
11. Harkness R, Simmonds R, Gough P, Priscott P, Squire J. Purine base and nucleoside, cytidine and uridine concentrations in foetal calf and other sera. Biochem Soc Trans. 1980;8:139.
12. Traut TW. Physiological concentrations of purines and pyrimidines. Mol Cell Biochem. 1994;140:1–22.
13. Tavazzi B, Lazzarino G, Leone P, Amorini AM, Bellia F, Janson CG, et al. Simultaneous high performance liquid chromatographic separation of purines, pyrimidines, N-acetylated amino acids, and dicarboxylic acids for the chemical diagnosis of inborn errors of metabolism. Clin Biochem. 2005;38:997–1008.
14. Alcorn N, Saunders S, Madhok R. Benefit-risk assessment of leflunomide: an appraisal of leflunomide in rheumatoid arthritis 10 years after licensing. Drug Saf. 2009;32:1123–1134.
15. Fairbanks LD, Bofill M, Ruckemann K, Simmonds HA. Importance of ribonucleotide availability to proliferating T-lymphocytes from healthy humans. Disproportionate expansion of pyrimidine pools and contrasting effects of de novo synthesis inhibitors. J Biol Chem. 1995;270:29682–29689.
16. Schmiedel BJ, Singh D, Madrigal A, Valdovino-Gonzalez AG, White BM, Zapardiel-Gonzalo J, et al. Impact of genetic polymorphisms on human immune cell gene expression. Cell. 2018;175:1701–1715.e16.
17. Gerner MC, Niederstaetter L, Ziegler L, Bileck A, Slany A, Janker L et al. Proteome analysis reveals distinct mitochondrial functions linked to interferon response patterns in activated CD4+ and CD8+ T Cells. Front Pharmacol. 2019;10.
18. Graessel A, Hauck SM, von Toerne C, Kloppmann E, Goldberg T, Koppensteiner H, et al. A combined omics approach to generate the surface atlas of human naive CD4+ T cells during Early T-cell receptor activation. Mol Cell Proteom MCP. 2015;14:2085–2102.
19. Ron-Harel N, Santos D, Ghergurovich JM, Sage PT, Reddy A, Lovitch SB, et al. Mitochondrial biogenesis and proteome remodeling promote one-carbon metabolism for T cell activation. Cell Metab. 2016;24:104–117.
20. Deng Y, Wang ZV, Gordillo R, An Y, Zhang C, Liang Q et al. An adipo-biliary-uridine axis that regulates energy homeostasis. Science. 2017;355.
21. Peters GJ. Re-evaluation of Brequinar sodium, a dihydroorotate dehydrogenase inhibitor. Nucleosides Nucleotides Nucleic Acids. 2018;37:666–678.

22. Cuthbertson CR, Guo H, Kyani A, Madak JT, Arabzada Z, Neamati N. The dihydroorotate dehydrogenase inhibitor brequinar is synergistic with ENT1/2 inhibitors. ACS Pharmacol Transl Sci. 2020;3:1242–1252.
23. Gaidano V, Houshmand M, Vitale N, Carrà G, Morotti A, Tenace V et al. The synergism between DHODH inhibitors and dipyridamole leads to metabolic lethality in acute myeloid leukemia. Cancers 2021;13.
24. Peters GJ, Kraal I, Pinedo HM. In vitro and in vivo studies on the combination of Brequinar sodium (DUP-785; NSC 368390) with 5-fluorouracil; effects of uridine. Br J Cancer. 1992;65:229–233.
25. Deans RM, Morgens DW, Ökesli A, Pillay S, Horlbeck MA, Kampmann M, et al. Parallel shRNA and CRISPR-Cas9 screens enable antiviral drug target identification. Nat Chem Biol. 2016;12:361–366.
26. Harenza JL, Diamond MA, Adams RN, Song MM, Davidson HL, Hart LS, et al. Transcriptomic profiling of 39 commonly-used neuroblastoma cell lines. Sci Data. 2017;4:170033.
27. Koundinya M, Sudhalter J, Courjaud A, Lionne B, Touyer G, Bonnet L, et al. Dependence on the pyrimidine biosynthetic enzyme DHODH is a synthetic lethal vulnerability in mutant KRAS-driven cancers. Cell Chem Biol 2018;25:705–717.e11.
28. Santana-Codina N, Roeth AA, Zhang Y, Yang A, Mashadova O, Asara JM, et al. Oncogenic KRAS supports pancreatic cancer through regulation of nucleotide synthesis. Nat Commun. 2018;9:4945.
29. Frances A, Cordelier P. The emerging role of cytidine deaminase in human diseases: a new opportunity for therapy? Mol Ther. 2020;28:357–366.
30. Peters GJ, Honeywell RJ, Maulandi M, Giovannetti E, Losekoot N, Etienne-Grimaldi M-C, et al. Selection of the best blood compartment to measure cytidine deaminase activity to stratify for optimal gemcitabine or cytarabine treatment. Nucleosides Nucleotides Nucleic Acids. 2014;33:403–412.
31. Wurtman RJ, Regan M, Ulus I, Yu L. Effect of oral CDP-choline on plasma choline and uridine levels in humans. Biochem Pharmacol. 2000;60:989–992.
32. Gareri P, Castagna A, Cotroneo AM, Putignano S, De Sarro G, Bruni AC. The role of citicoline in cognitive impairment: pharmacological characteristics, possible advantages, and doubts for an old drug with new perspectives. Clin Interv Aging. 2015;10:1421–1429.
33. Peters GJ, van Groeningen CJ, Laurensse EJ, Lankelma J, Leyva A, Pinedo HM. Uridine induced hypothermia in mice and rats in relation to plasma and tissue levels of uridine and its metabolites. Cancer Chemother Pharmacol. 1988;21:268–268.
34. Peters GJ, van Groeningen CJ, Laurensse E, Kraal I, Leyva A, Lankelma J, et al. Effect of pyrimidine nucleosides on body temperatures of man and rabbit in relation to pharmacokinetic data. Pharm Res. 1987;4:113–119.
35. Xiao C, Liu N, Jacobson KA, Gavrilova O, Reitman ML. Physiology and effects of nucleosides in mice lacking all four adenosine receptors. PLoS Biol. 2019;17:e3000161.
36. Cohen R, Preta LH, Joste V, Curis E, Huillard O, Jouinot A, et al. Determinants of the interindividual variability in serum cytidine deaminase activity of patients with solid tumours. Br J Clin Pharmacol. 2019;85:1227–1238.
37. Farrell JJ, Bae K, Wong J, Guha C, Dicker AP, Elsaleh H. Cytidine deaminase single-nucleotide polymorphism is predictive of toxicity from gemcitabine in patients with pancreatic cancer: RTOG 9704. Pharmacogenomics J. 2012;12:395–403.
38. Kronbichler A, Brezina B, Quintana LF, Jayne DRW. Efficacy of plasma exchange and immunoadsorption in systemic lupus erythematosus and antiphospholipid syndrome: a systematic review. Autoimmun Rev. 2016;15:38–49.
39. Thompson PW, Jones DD, Currey HL. Cytidine deaminase activity as a measure of acute inflammation in rheumatoid arthritis. Ann Rheum Dis. 1986;45:9–14.
40. Taysi S, Polat MF, Sari RA, Bakan E. Serum adenosine deaminase and cytidine deaminase activities in patients with systemic lupus erythematosus. Clin Chem Lab Med. 2002;40:493–495.
41. Yu CL, Tsai CY, Sun KH, Chen YS, Lin WM, Liao TS, et al. Increased spontaneous release of cytidine deaminase by polymorphonuclear neutrophils of patients with active systemic lupus erythematosus. Br J Rheumatol. 1992;31:675–678.
42. Thompson PW, James IT, Wheatcroft S, Pownall R, Barnes CG. Circadian rhythm of serum cytidine

deaminase in patients with rheumatoid arthritis during rest and exercise. Ann Rheum Dis. 1989;48:502–504.

43. Lahoz-Beneytez J, Elemans M, Zhang Y, Ahmed R, Salam A, Block M, et al. Human neutrophil kinetics: modeling of stable isotope labeling data supports short blood neutrophil half-lives. Blood. 2016;127:3431–3438.
44. Jeong J, Suh Y, Jung K. Context drives diversification of monocytes and neutrophils in orchestrating the tumor microenvironment. Front Immunol. 2019;10:1817.
45. Uribe-Querol E, Rosales C. Neutrophils in cancer: two sides of the same coin. J Immunol Res. 2015;2015:e983698.
46. O'Connell KE, Mikkola AM, Stepanek AM, Vernet A, Hall CD, Sun CC, et al. Practical murine hematopathology: a comparative review and implications for research. Comp Med. 2015;65:96–113.
47. Bøyum A, Tennfjord V-A, Gran C, Løvhaug D, Øktedalen O, Brandtzaeg P. Bioactive cytidine deaminase, an inhibitor of granulocyte-macrophage colony-forming cells, is massively released in fulminant meningococcal sepsis. J Infect Dis. 2000;182:1784–1787.
48. Sohal D, Krishnamurthi S, Tohme R, Gu X, Lindner D, Landowski TH, et al. A pilot clinical trial of the cytidine deaminase inhibitor tetrahydrouridine combined with decitabine to target DNMT1 in advanced, chemorefractory pancreatic cancer. Am J Cancer Res. 2020;10:3047–3060.